



Possible chiral doublets in ^{60}Ni

J. Peng^{a,*}, Q.B. Chen^b

^a Department of Physics, Beijing Normal University, Beijing 100875, China

^b Physik-Department, Technische Universität München, D-85747 Garching, Germany



ARTICLE INFO

Article history:

Received 26 December 2018

Received in revised form 20 April 2019

Accepted 26 April 2019

Available online 2 May 2019

Editor: W. Haxton

ABSTRACT

The open problem on whether or not the chirality exists in doublet bands M1 and M4 in light-mass even-even nucleus ^{60}Ni is studied by adopting the recently developed fully quantal four- j shells triaxial particle rotor model. The corresponding experimental energy spectra, energy differences between doublet bands, and the available $B(M1)/B(E2)$ values are successfully reproduced. The analyses on the basis of the angular momentum components, the azimuthal plots, and the K -plots suggest that the chiral modes exist at $I \geq 12 \hbar$ in doublet bands M1 and M4.

© 2019 The Authors. Published by Elsevier B.V. This is an open access article under the CC BY license (<http://creativecommons.org/licenses/by/4.0/>). Funded by SCOAP³.

Nuclear chiral rotation is an exotic form of spontaneous symmetry breaking, which exists only in nucleus with triaxial ellipsoidal shape. In 1997, Frauendorf and Meng proposed that the total angular momentum vector of a rotating triaxial nucleus may lie outside the three principal planes in the intrinsic frame. Such an angular momentum geometry can, in the laboratory frame, give rise to a pair of nearly degenerate $\Delta I = 1$ bands with the same parity, i.e., chiral doublet bands [1]. So far, more than 50 chiral candidates have been reported in odd-odd, odd- A , and even-even nuclei that spread over $A \sim 80$ [2], 100 [3–10], 130 [11–21], and 190 mass regions [22,23]. For more details, see reviews [24–29] and very recent data tables [30].

During the process of investigating nuclear chirality, exploring novel chiral phenomena and searching for new chiral candidates are the two fundamental goals all the time. For the former, e.g., the multiple chiral doublets ($M \times D$) phenomenon, i.e., having multiple pairs of chiral doublet bands in a single nucleus, was theoretically predicted and explored by the state-of-art covariant density functional theory (CDFT) [31–37] and observed in ^{133}Ce [38], ^{103}Rh [39], ^{78}Br [40], ^{136}Nd [41,42], and ^{195}Tl [43]. These observations confirm the existence of triaxial shapes coexistence [31,38,41,43], and reveal the stability of chiral geometry against the increasing of intrinsic excitation energy [39,44–47] and octupole correlations [40]. For the latter, the experimental evidence of chiral doublet bands was first observed in the $A \sim 130$ mass region, and then followed by the $A \sim 100$, 190, and 80 mass regions. These observations show that the nuclear chirality is not a specific phenomenon that exists in only one nucleus or one mass region.

Both of the two fundamental goals and all of relevant observations mentioned above encourage us to search for new candidates with chirality or $M \times D$ in new mass regions. In Ref. [37], we explored the $M \times D$ in $A \sim 60$ mass region by the adiabatic and configuration-fixed constrained CDFT for cobalt isotopes. It was found that there are high- j particle(s) and hole(s) configurations with prominent triaxially deformed shapes in these isotopes, which suggests the possibility of chirality or multiple chirality in $A \sim 60$ mass region. However, the experimental energy spectra and electromagnetic transition in these isotopes are rather rare at present.

We note that in Ref. [48], the fully microscopic self-consistent tilted axis cranking covariant density functional theory (TAC-CDFT) was applied to investigate the observed dipole bands M1, M2, M3, and M4 in even-even nucleus ^{60}Ni [49]. It was mentioned that bands M1 and M4 might be the possible candidates for chiral doublet bands. However, due to the mean-field approximation, the TAC can only give the description for the band M1. After that, there is neither further theoretical nor experimental work to investigate bands M1 and M4 in ^{60}Ni . Therefore, whether the chirality exists in the bands M1 and M4 or not is still an open problem.

The aim of the present work is to investigate the chirality in doublet bands M1 and M4 in ^{60}Ni in a fully quantal model. As a quantal model coupling the collective rotation and the single-particle motions, the particle rotor model (PRM) has been widely used to describe the chiral doublet bands and achieved major successes [24]. In contrast to the TAC approach, PRM describes a system in the laboratory frame. The total Hamiltonian is diagonalized with total angular momentum as a good quantum number, and the energy splitting and quantum tunneling between the doublet bands can be obtained directly. Moreover, the basic microscopic

* Corresponding author.

E-mail addresses: jpeng@bnu.edu.cn (J. Peng), qbchen@pku.edu.cn (Q.B. Chen).

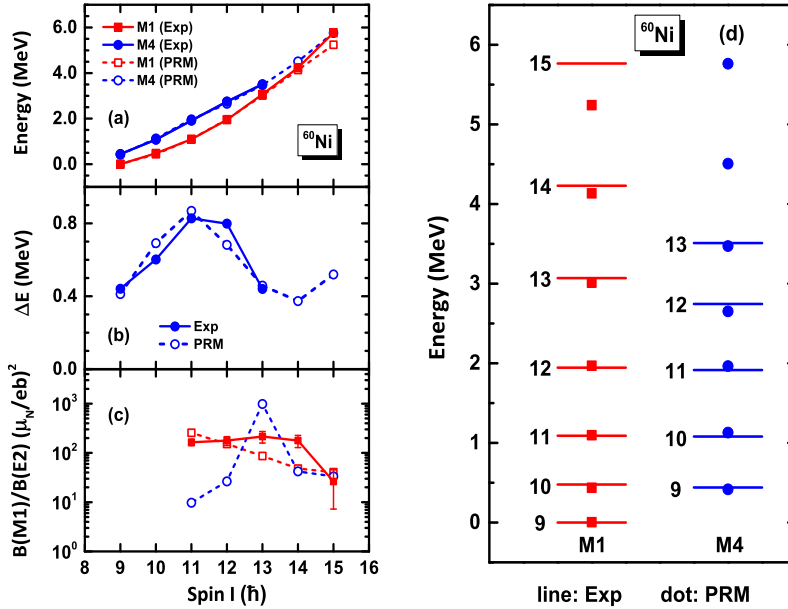


Fig. 1. (a) Energy spectra as functions of spin for the bands M1 and M4 in ^{60}Ni calculated by PRM in comparison with the data. (b) Theoretical and experimental energy difference between the doublet bands. (c) $B(\text{M}1)/B(\text{E}2)$ of bands M1 and M4 calculated by PRM in comparison with the available data. (d) Energy level scheme of bands M1 and M4.

inputs for PRM can be obtained from the constrained CDFT [9, 31,38–40,50,51]. Various versions of PRM have been developed to investigate the chiral doublet bands with different kinds of configurations [1,9,16,23,38,39,47,51–64]. To describe the doublet bands M1 and M4 in ^{60}Ni with four quasi-particle configuration [48,49], a four- j shell PRM is needed. Such version of PRM has already been developed very recently and applied to describe the M χ D in ^{136}Nd [42].

In this letter, the four- j shell PRM will be applied to study the energy spectra and the electromagnetic transition probabilities of the doublet bands M1 and M4 in ^{60}Ni , and to explore the open problem on whether or not the chirality exists in this doublet by examining their angular momentum geometries.

The formalism of PRM with four- j shell can be found in Ref. [42]. The total wave function of PRM Hamiltonian is expanded into the strong coupling basis

$$|IM\rangle = \sum_{K\phi} c_{K\phi} |IMK\phi\rangle, \quad (1)$$

with

$$|IMK\phi\rangle = \frac{1}{\sqrt{2(1 + \delta_{K0}\delta_{\phi,\bar{\phi}})}} \times (|IMK\rangle|\phi\rangle + (-1)^{I-K}|IM-K\rangle|\bar{\phi}\rangle), \quad (2)$$

where $|IMK\rangle$ is the Wigner function $\sqrt{\frac{2I+1}{8\pi^2}} D_{MK}^I$, $|\phi\rangle$ is the product of the proton and neutron states those sitting in the four- j shells, and the $c_{K\phi}$ is the expansion coefficient obtained by diagonalizing the PRM Hamiltonian. With the obtained wave functions, the reduced transition probabilities $B(\text{M}1)$ and $B(\text{E}2)$ can be calculated [65]. In addition, one can also calculate the expectation values of the angular momentum components [42,62],

$$J_k = \sqrt{\langle IM|\hat{J}_k^2|IM\rangle}, \quad (3)$$

the probability distributions of the total angular momentum in the intrinsic reference frame (azimuthal plot) [56,66,67],

$$\begin{aligned} \mathcal{P}(\theta, \varphi) = 2\pi \sum_{\phi'} & \left| \sum_{K,\phi} c_{K\phi} \sqrt{\frac{2I+1}{16\pi^2}} [D_{IK}^I(\psi, \theta, \pi - \varphi) \delta_{\phi',\phi} \right. \\ & \left. + (-1)^{I-K} D_{I-K}^I(\psi, \theta, \pi - \varphi) \delta_{\phi',-\phi}] \right|^2, \end{aligned} \quad (4)$$

and the probability distributions of the total angular momentum components on the three principle axes (K -plot) [62,66],

$$P_K = \sum_{\phi} |c_{K\phi}|^2. \quad (5)$$

Based on these analyses, one can study the angular momentum geometries systematically to make an unambiguous judgment whether or not the chiral geometry exists in the doublet bands.

In the PRM calculations for the doublet bands M1 and M4 in ^{60}Ni , the configuration $\pi(1f_{7/2})^{-1}(2p_{3/2})^1 \otimes \nu(1g_{9/2})^1(1f_{5/2})^{-1}$ [48,49] is adopted. The deformation parameters $\beta = 0.27$ and $\gamma = 19^\circ$ for this configuration at the bandhead were obtained from the microscopic self-consistent TAC-CDFT calculations [48]. With the rotation, the β value decreases smoothly, while γ value shows a smoothly increasing tendency. In the PRM calculation, the deformation parameters are fixed. To reproduce the energy spectra better, we use a deformation of $\beta = 0.27$ and $\gamma = 22^\circ$. The moment of inertia $J_0 = 9.0 \text{ } \hbar^2/\text{MeV}$ and Coriolis attenuation factor $\xi = 0.98$ are adopted according to the experimental energy spectra. For the electromagnetic transitions, the empirical intrinsic quadrupole moment $Q_0 = (3/\sqrt{5\pi}) R_0^2 Z \beta$, and gyromagnetic ratios for rotor $g_R = Z/A$ and for nucleons $g_{p(n)} = g_l + (g_s - g_l)/(2l+1)$ ($g_l = 1(0)$ for protons (neutrons) and $g_s = 0.6g_s(\text{free})$) [68] are adopted.

The calculated energy spectra for the bands M1 and M4 in ^{60}Ni are presented in Fig. 1(a), together with the corresponding data. The experimental energy spectra are reproduced excellently by the PRM calculations. Such a good agreement can be more clearly seen by showing the energy level scheme in Fig. 1(d).

Being a fully quantal model, PRM is capable of reproducing the energy splitting ΔE between the doublet bands for the whole observed spin region. This is illustrated in Fig. 1(b). The ΔE increases firstly from $I = 9$ to $11 \text{ } \hbar$, and then decreases up to $I = 14 \text{ } \hbar$. At

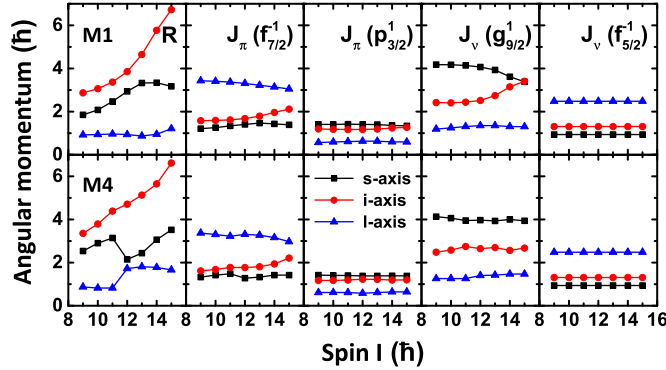


Fig. 2. The root mean square components along the short (*s*-, squares), intermediate (*i*-, circles), and long (*l*-, triangles) axes of the rotor, valence protons, and valence neutrons angular momenta calculated as functions of spin by PRM for the doublet bands M1 and M4 in ^{60}Ni .

$I = 15 \hbar$, an increasing trend is observed once again in the PRM results. It is known that in an ideal chiral system with the particle-hole configuration $\pi(1h_{11/2})^1 \otimes \nu(1h_{11/2})^{-1}$ and a rotor with the deformation parameter $\gamma = 30^\circ$, the ΔE is small (less than 400 keV) and shows a trend that decreases firstly and then increases [1,56]. Here, at $I \geq 12 \hbar$, the ΔE shows the similar variation trend, giving a hint that chirality might exist in bands M1 and M4. The large ΔE (higher than 400 keV) could be owed to the small triaxial deformation [47,54]. Therefore, it would be very interesting to extend the spectrum of band M4, which only reaches to $I = 13 \hbar$ currently, to higher spins to further verify the theoretical calculations.

In Fig. 1(c), the $B(M1)/B(E2)$ values of bands M1 and M4 calculated by PRM in comparison with the available data are shown. One observes that the PRM calculations show a good agreement with the data at $I = 11$ and $12 \hbar$ for band M1. At $I = 13$ and $14 \hbar$, the calculated $B(M1)/B(E2)$ is smaller than the data. This is because the decrease of β with the rotation [48] is not taken into account in the present PRM calculations. The calculated $B(M1)/B(E2)$ for band M4 at $I = 13 \hbar$ is very large. It is caused by, as shown later, the wave function structure changes dramatically from $I = 12$ to $13 \hbar$. The calculated $B(M1)/B(E2)$ values of bands M1 and M4 at $I = 14$ and $15 \hbar$ are similar, which further implies the chirality exists. Therefore, further experimental efforts on extracting electromagnetic transition data for band M4 are highly demanded to obtain solid evidence.

The rotational motion of triaxial nuclei attains a chiral character if the angular momentum has substantial projections on all three principal axes of the triaxially deformed nucleus [1]. The successes in reproducing the energy spectra and available electromagnetic transition probabilities for the doublet bands M1 and M4 in ^{60}Ni motivate us to investigate the expectation values of the squared angular momentum components along the short (*s*-), intermediate (*i*-), and long (*l*-)axes for the rotor, valence protons, and valence neutrons. As shown in Fig. 2, the substantial projections of angular momentum on three principal axes can be observed for bands M1 and M4.

For both bands M1 and M4, the collective core angular momentum mainly aligns along the *i*-axis in the whole spin region, because it has the largest moment of inertia. In band M4, the *s*- and *l*-components of the rotor angular momentum exhibit discontinuous behaviors from $I = 11$ to $12 \hbar$. This is understood as the reason of abrupt increases of $B(M1)/B(E2)$ values, as discussed previously. The angular momenta of the $f_{7/2}$ valence proton and $f_{5/2}$ valence neutron holes mainly align along the *l*-axis, and that of valence neutron $g_{9/2}$ particle mainly along the *s*-axis. At high

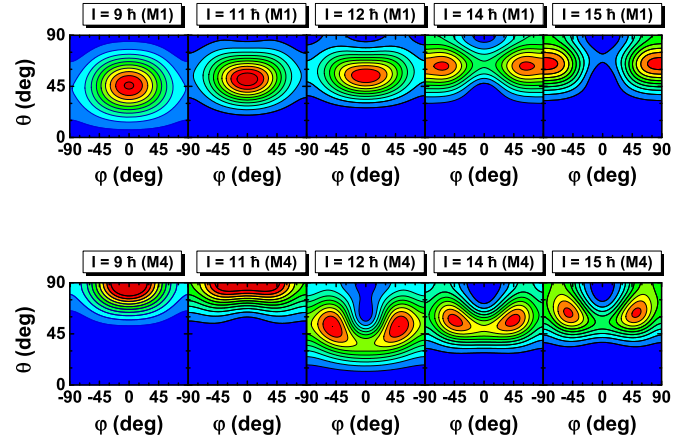


Fig. 3. The azimuthal plots, i.e., profiles for the orientation of the angular momentum on the (θ, φ) plane calculated by PRM at $I = 9, 11, 12, 14$, and $15 \hbar$ for the doublet bands M1 and M4 in ^{60}Ni .

spin region in band M1, the *i*-component (*s*-component) of $g_{9/2}$ particle gradually increases (decreases). For $p_{3/2}$ proton, the *s*- and *i*-components are similar to each other. Such orientations form the chiral geometry of aplanar rotation.

The spontaneous chiral symmetry breaking or chiral geometry is realized by the total angular momentum lying outside the three principal planes in the intrinsic frame [1]. In order to visualize the angular momentum geometry in the intrinsic frame, the azimuthal plots [56,66,67], i.e., profiles $P(\theta, \varphi)$ for the orientation of the angular momentum on the (θ, φ) plane calculated by PRM using Eq. (4) are shown in Fig. 3 for the doublet bands M1 and M4 in ^{60}Ni at $I = 9, 11, 12, 14$, and $15 \hbar$. We emphasize that θ is the angle between the total spin \mathbf{I} and the *l*-axis, and φ is the angle between the projection of \mathbf{I} onto the *si*-plane and the *s*-axis. As is shown in Fig. 3, the azimuthal plots are symmetric with respect to $\varphi = 0^\circ$. This is because the broken chiral symmetry in the intrinsic frame has been restored in PRM.

For $I = 9$ (bandhead) and $11 \hbar$ (kink of ΔE), the profiles for the orientation of the angular momentum for band M1 have only one single peak at $(\theta \sim 45^\circ, \varphi = 0^\circ)$, which suggests that the angular momentum stays within the *sl*-plane. Instead, the profiles for band M4 peak at $(\theta = 90^\circ, \varphi = 0^\circ)$, corresponding to a principal axis rotation with respect to *s*-axis. Such two orientations do not form a chiral geometry. Therefore, no chirality is shown for $I = 9-11 \hbar$. This is also the reason why the energy splitting ΔE increases at this spin region, as shown in Fig. 1(b).

For $I = 12 \hbar$, the profile for band M1 still peaks at $\varphi = 0^\circ$. However, that for band M4 shows a node around $(\theta \sim 60^\circ, \varphi = 0^\circ)$ with the onset of two peaks locating at $(\theta \sim 45^\circ, \varphi \sim 45^\circ)$ and $(\theta \sim 45^\circ, \varphi \sim -45^\circ)$, respectively. The appearances of node and two peaks are consistent with the picture of a 0-phonon state in band M1 and 1-phonon vibration in band M4 [56,66,67]. Therefore, the chiral vibration is demonstrated for $I = 12 \hbar$. Due to the chiral vibration, the *i*- (*s*-) component of the rotator angular momentum at $I = 12 \hbar$ for band M4 is larger (smaller) than that for band M1, as shown in Fig. 2.

For $I = 14 \hbar$, two peaks corresponding to aplanar orientations are found in the both of doublet bands, i.e., $(\theta \sim 60^\circ, \varphi \sim 60^\circ)$ and $(\theta \sim 60^\circ, \varphi \sim -60^\circ)$ for band M1, while $(\theta \sim 55^\circ, \varphi \sim 50^\circ)$ and $(\theta \sim 55^\circ, \varphi \sim -50^\circ)$ for band M4. These features could be understood as a realization of static chirality, and hence give the lowest ΔE as shown in Fig. 1(b).

For $I = 15 \hbar$, the peaks for band M1 move toward to $(\theta \sim 60^\circ, \varphi \sim 90^\circ)$ and $(\theta \sim 60^\circ, \varphi \sim -90^\circ)$, namely in the *il*-plane and close to *i*-axis. This is mainly driven by the gradual increasing

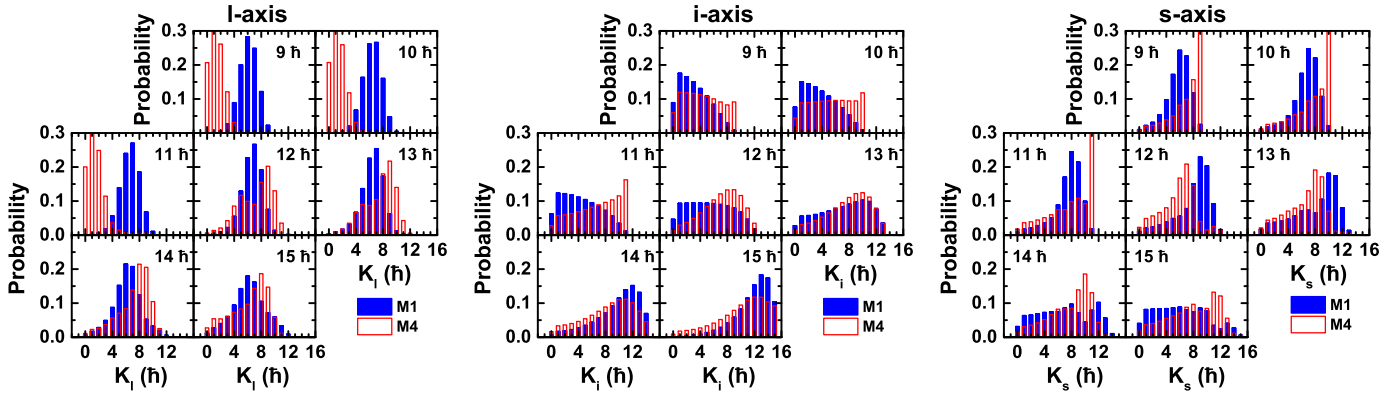


Fig. 4. The K -plots, i.e., K -distributions for the angular momentum on the long (l)-, intermediate (i)-, and short (s)-axes calculated by PRM for the doublet bands M1 and M4 in ^{60}Ni .

of i -components of the rotor, and valence neutron $g_{9/2}$ particle, and valence proton $f_{7/2}$ hole angular momenta, as presented in Fig. 2. The peaks for the azimuthal plot for band M4 locate at $(\theta \sim 60^\circ, \varphi \sim 60^\circ)$ and $(\theta \sim 60^\circ, \varphi \sim -60^\circ)$. At this spin, bands M1 and M4 attain vibration character again, which is now with respect to il -plane. As a consequence, their energy difference ΔE , as shown in Fig. 1(b), increases [69,70].

To further understand the evolution of the chirality with spin, in Fig. 4, the K -plots, i.e., K -distributions for the angular momentum on the l -, i -, and s -axes calculated by PRM for the doublet bands M1 and M4 in ^{60}Ni are displayed. As seen in the figures, the evolutions of the rotational modes from no chirality at $I = 9-11 \hbar$, to the chiral vibration at $I = 12 \hbar$, then to the static chirality at $I = 13-14 \hbar$, and finally to the second vibration at $I = 15 \hbar$ are exhibited clearly.

For $I = 9-11 \hbar$, the peaks of K_l locate around $K_l = 6 \hbar$ for band M1, while at $K_l = 1 \hbar$ for band M4. The K_l -distribution peaks at $K_l = 1 \hbar$ for band M1, while spreads widely for band M4. The K_s -distributions of both bands peak at large K_s value. All of these are in accordance with the features observed in the azimuthal plots shown in Fig. 3. Namely, the angular momentum of band M1 stays within the sl -plane, while that of band M4 aligns along s -axis.

For $I = 12 \hbar$, K_l distribution of band M4 shows a rapid change, which is caused by the discontinuous variation of the l -component of rotor angular momentum, as shown in Fig. 2. The K_l -distribution spreads around $K_l = 0$ for band M1, whereas it almost vanishes for band M4. This is in accordance with the interpretation of the chiral vibration with respect to the sl -plane where the zero-phonon state (band M1) is symmetric with respect to $K_l = 0$ and the one-phonon state (band M4) is antisymmetric.

For $I = 13$ and $14 \hbar$, the K_l -distributions of bands M1 and M4 are rather similar. The position of peak of K_l - (K_s) distribution for band M1 is a bit smaller (larger) than those for band M4. Such differences lead the different azimuthal plots shown in Fig. 3 and lead that the energy splitting of bands M1 and M4 is a bit large (~ 400 keV), though they are, in fact, in the static chirality region.

For $I = 15 \hbar$, the K_l - and K_i -distributions for bands M1 and M4 are similar. However, for the K_s -distribution, they are different. The most probable value spreads at $K_s \sim 1 \hbar$ for band M1, while appears at $K_s \sim 11 \hbar$ for band M4. This further supports the appearance of second chiral vibration with respect to il -plane.

In summary, the open problem on whether or not the chirality exists in doublet bands M1 and M4 in light-mass even-even nucleus ^{60}Ni is studied by adopting the recently developed fully quantal four- j shells triaxial particle rotor model. The corresponding experimental energy spectra, energy differences between the

doublet bands, and the available $B(M1)/B(E2)$ values are successfully reproduced. The analyses based on the angular momentum components, the azimuthal plots, and the K -plots suggest that the chiral modes exist at $I \geq 12 \hbar$. Namely, there is no indication of chirality at $I \leq 11 \hbar$. A chiral vibration appears at $I = 12 \hbar$, then changes to nearly static chirality at $I = 14 \hbar$, and finally evolves to another type of chiral vibration at $I = 15 \hbar$.

Further experimental efforts on extending the level scheme and extracting electromagnetic transition data for band M4 are highly demanded to obtain solid evidence. According to current investigation, we would also like to attract more experimental and theoretical efforts on the investigation of chirality or multiple chirality in the $A \sim 60$ mass region and even in the lighter-mass region.

Acknowledgements

The authors thank Professor Jie Meng for helpful discussions. This work is supported by the National Natural Science Foundation of China (NSFC) under Grants No. 11775026 and 11875027, and the Deutsche Forschungsgemeinschaft (DFG) and NSFC through funds provided to the Sino-German CRC110 “Symmetries and the Emergence of Structure in QCD” (DFG Grant No. TRR110 and NSFC Grant No. 11621131001).

References

- [1] S. Frauendorf, J. Meng, Nucl. Phys. A 617 (1997) 131.
- [2] S.Y. Wang, B. Qi, L. Liu, S.Q. Zhang, H. Hua, X.Q. Li, Y.Y. Chen, L.H. Zhu, J. Meng, S.M. Wyngaardt, et al., Phys. Lett. B 703 (2011) 40.
- [3] C. Vaman, D.B. Fossan, T. Koike, K. Starosta, I.Y. Lee, A.O. Macchiavelli, Phys. Rev. Lett. 92 (2004) 032501.
- [4] P. Joshi, D.G. Jenkins, P.M. Raddon, A.J. Simons, R. Wadsworth, A.R. Wilkinson, D.B. Fossan, T. Koike, K. Starosta, C. Vaman, et al., Phys. Lett. B 595 (2004) 135.
- [5] J. Timár, P. Joshi, K. Starosta, V.I. Dimitrov, D.B. Fossan, J. Molnar, D. Sohler, R. Wadsworth, A. Algora, P. Bednarczyk, et al., Phys. Lett. B 598 (2004) 178.
- [6] J.A. Alcántara-Núñez, J.R.B. Oliveira, E.W. Cybulski, N.H. Medina, M.N. Rao, R.V. Ribas, M.A. Rizzutto, W.A. Seale, F. Falla-Sotelo, K.T. Wiedemann, et al., Phys. Rev. C 69 (2004) 024317.
- [7] Y.X. Luo, S.J. Zhu, J.H. Hamilton, J.O. Rasmussen, A.V. Ramayya, C. Goodin, K. Li, J.K. Hwang, D. Almeined, S. Frauendorf, et al., Phys. Lett. B 670 (2009) 307.
- [8] D. Tonev, M.S. Yavahchova, N. Goutev, G. de Angelis, P. Petkov, R.K. Bhownik, R.P. Singh, S. Muralithar, N. Madhavan, R. Kumar, et al., Phys. Rev. Lett. 112 (2014) 052501.
- [9] E.O. Lieder, R.M. Lieder, R.A. Bark, Q.B. Chen, S.Q. Zhang, J. Meng, E.A. Lawrie, J.J. Lawrie, S.P. Bvumbi, N.Y. Kheswa, et al., Phys. Rev. Lett. 112 (2014) 202502.
- [10] B. Moon, C.-B. Moon, G. Dracoulis, R. Bark, A. Byrne, P. Davidson, G. Lane, T. Kibédi, A. Wilson, C. Yuan, et al., Phys. Lett. B 782 (2018) 602.
- [11] K. Starosta, T. Koike, C.J. Chiara, D.B. Fossan, D.R. LaFosse, A.A. Hecht, C.W. Beausang, M.A. Caprio, J.R. Cooper, R. Krücken, et al., Phys. Rev. Lett. 86 (2001) 971.
- [12] T. Koike, K. Starosta, C.J. Chiara, D.B. Fossan, D.R. LaFosse, Phys. Rev. C 63 (2001) 061304.

- [13] A.A. Hecht, C.W. Beausang, K.E. Zyromski, D.L. Balabanski, C.J. Barton, M.A. Caprio, R.F. Casten, J.R. Cooper, D.J. Hartley, R. Krucken, et al., Phys. Rev. C 63 (2001) 051302.
- [14] D.J. Hartley, L.L. Riedinger, M.A. Riley, D.L. Balabanski, F.G. Kondev, R.W. Laird, J. Pfohl, D.E. Archer, T.B. Brown, R.M. Clark, et al., Phys. Rev. C 64 (2001) 031304.
- [15] S. Zhu, U. Garg, B.K. Nayak, S.S. Ghugre, N.S. Pattabiraman, D.B. Fossan, T. Koike, K. Starosta, C. Vaman, R.V.F. Janssens, et al., Phys. Rev. Lett. 91 (2003) 132501.
- [16] T. Koike, K. Starosta, C.J. Chiara, D.B. Fossan, D.R. LaFosse, Phys. Rev. C 67 (2003) 044319.
- [17] E. Grodner, J. Srebrny, A.A. Pasternak, I. Zalewska, T. Morek, C. Droste, J. Mierzejewski, M. Kowalczyk, J. Kownacki, M. Kisielinski, et al., Phys. Rev. Lett. 97 (2006) 172501.
- [18] S.Y. Wang, Y.Z. Liu, I. Komatsubara, Y.J. Ma, Y.H. Zhang, Phys. Rev. C 74 (2006) 017302.
- [19] S. Mukhopadhyay, D. Almehed, U. Garg, S. Frauendorf, T. Li, P.V.M. Rao, X. Wang, S.S. Ghugre, M.P. Carpenter, S. Gros, et al., Phys. Rev. Lett. 99 (2007) 172501.
- [20] E. Grodner, I. Sankowska, T. Morek, S.G. Rohozinski, C. Droste, J. Srebrny, A.A. Pasternak, M. Kisielinski, M. Kowalczyk, J. Kownacki, et al., Phys. Lett. B 703 (2011) 46.
- [21] M. Ionescu-Bujor, S. Aydin, N. Mărginean, C. Costache, D. Bucurescu, N. Florea, T. Glodariu, A. Ionescu, A. Iordăchescu, R. Mărginean, et al., Phys. Rev. C 98 (2018) 054305.
- [22] D.L. Balabanski, M. Danchev, D.J. Hartley, L.L. Riedinger, O. Zeidan, J.-y. Zhang, C.J. Barton, C.W. Beausang, M.A. Caprio, R.F. Casten, et al., Phys. Rev. C 70 (2004) 044305.
- [23] E.A. Lawrie, P.A. Vymers, J.J. Lawrie, C. Vieu, R.A. Bark, R. Lindsay, G.K. Mabala, S.M. Maliage, P.L. Masiteng, S.M. Mullins, et al., Phys. Rev. C 78 (2008) 021305.
- [24] J. Meng, S.Q. Zhang, J. Phys. G, Nucl. Part. Phys. 37 (2010) 064025.
- [25] J. Meng, Q.B. Chen, S.Q. Zhang, Int. J. Mod. Phys. E 23 (2014) 1430016.
- [26] R.A. Bark, E.O. Lieder, R.M. Lieder, E.A. Lawrie, J.J. Lawrie, S.P. Bvumbi, N.Y. Kheswa, S.S. Ntshangase, T.E. Madiba, P.L. Masiteng, et al., Int. J. Mod. Phys. E 23 (2014) 1461001.
- [27] J. Meng, P.W. Zhao, Phys. Scr. 91 (2016) 053008.
- [28] A.A. Raduta, Prog. Part. Nucl. Phys. 90 (2016) 241.
- [29] S. Frauendorf, Phys. Scr. 93 (2018) 043003.
- [30] B.W. Xiong, Y.Y. Wang, At. Data Nucl. Data Tables 125 (2019) 193.
- [31] J. Meng, J. Peng, S.Q. Zhang, S.-G. Zhou, Phys. Rev. C 73 (2006) 037303.
- [32] J. Peng, H. Sagawa, S.Q. Zhang, J.M. Yao, Y. Zhang, J. Meng, Phys. Rev. C 77 (2008) 024309.
- [33] J.M. Yao, B. Qi, S.Q. Zhang, J. Peng, S.Y. Wang, J. Meng, Phys. Rev. C 79 (2009) 067302.
- [34] J. Li, S.Q. Zhang, J. Meng, Phys. Rev. C 83 (2011) 037301.
- [35] J. Li, Phys. Rev. C 97 (2018) 034306.
- [36] B. Qi, H. Jia, C. Liu, S.Y. Wang, Phys. Rev. C 98 (2018) 014305.
- [37] J. Peng, Q.B. Chen, Phys. Rev. C 98 (2018) 024320.
- [38] A.D. Ayangeakaa, U. Garg, M.D. Anthony, S. Frauendorf, J.T. Matta, B.K. Nayak, D. Patel, Q.B. Chen, S.Q. Zhang, P.W. Zhao, et al., Phys. Rev. Lett. 110 (2013) 172504.
- [39] I. Kuti, Q.B. Chen, J. Timár, D. Sohler, S.Q. Zhang, Z.H. Zhang, P.W. Zhao, J. Meng, K. Starosta, T. Koike, et al., Phys. Rev. Lett. 113 (2014) 032501.
- [40] C. Liu, S.Y. Wang, R.A. Bark, S.Q. Zhang, J. Meng, B. Qi, P. Jones, S.M. Wyngaardt, J. Zhao, C. Xu, et al., Phys. Rev. Lett. 116 (2016) 112501.
- [41] C.M. Petrache, B.F. Lv, A. Astier, E. Dupont, Y.K. Wang, S.Q. Zhang, P.W. Zhao, Z.X. Ren, J. Meng, P.T. Greenlees, et al., Phys. Rev. C 97 (2018) 041304(R).
- [42] Q.B. Chen, B.F. Lv, C.M. Petrache, J. Meng, Phys. Lett. B 782 (2018) 744.
- [43] T. Roy, G. Mukherjee, M. Asgar, S. Bhattacharyya, S. Bhattacharya, C. Bhattacharya, S. Bhattacharya, T. Ghosh, K. Banerjee, S. Kundu, et al., Phys. Lett. B 782 (2018) 768.
- [44] C. Droste, S.G. Rohozinski, K. Starosta, L. Prochniak, E. Grodner, Eur. Phys. J. A 42 (2009) 79.
- [45] Q.B. Chen, J.M. Yao, S.Q. Zhang, B. Qi, Phys. Rev. C 82 (2010) 067302.
- [46] I. Hamamoto, Phys. Rev. C 88 (2013) 024327.
- [47] H. Zhang, Q.B. Chen, Chin. Phys. C 40 (2016) 024101.
- [48] P.W. Zhao, S.Q. Zhang, J. Peng, H.Z. Liang, P. Ring, J. Meng, Phys. Lett. B 699 (2011) 181.
- [49] D.A. Torres, F. Cristancho, L.-L. Andersson, E.K. Johansson, D. Rudolph, C. Fahlander, J. Ekman, R. du Rietz, C. Andreoiu, M.P. Carpenter, et al., Phys. Rev. C 78 (2008) 054318.
- [50] J. Meng (Ed.), Relativistic Density Functional for Nuclear Structure, International Review of Nuclear Physics, vol. 10, World Scientific, Singapore, 2016.
- [51] C.M. Petrache, Q.B. Chen, S. Guo, A.D. Ayangeakaa, U. Garg, J.T. Matta, B.K. Nayak, D. Patel, J. Meng, M.P. Carpenter, et al., Phys. Rev. C 94 (2016) 064309.
- [52] J. Peng, J. Meng, S.Q. Zhang, Phys. Rev. C 68 (2003) 044324.
- [53] T. Koike, K. Starosta, I. Hamamoto, Phys. Rev. Lett. 93 (2004) 172502.
- [54] B. Qi, S.Q. Zhang, S.Y. Wang, J.M. Yao, J. Meng, Phys. Rev. C 79 (2009) 041302(R).
- [55] Q.B. Chen, K. Starosta, T. Koike, Phys. Rev. C 97 (2018) 041303(R).
- [56] Q.B. Chen, J. Meng, Phys. Rev. C 98 (2018) 031303.
- [57] S.Q. Zhang, B. Qi, S.Y. Wang, J. Meng, Phys. Rev. C 75 (2007) 044307.
- [58] S.Y. Wang, S.Q. Zhang, B. Qi, J. Meng, Phys. Rev. C 75 (2007) 024309.
- [59] S.Y. Wang, S.Q. Zhang, B. Qi, J. Peng, J.M. Yao, J. Meng, Phys. Rev. C 77 (2008) 034314.
- [60] E.A. Lawrie, O. Shirinda, Phys. Lett. B 689 (2010) 66.
- [61] O. Shirinda, E.A. Lawrie, Eur. Phys. J. A 48 (2012) 118.
- [62] B. Qi, S.Q. Zhang, J. Meng, S.Y. Wang, S. Frauendorf, Phys. Lett. B 675 (2009) 175.
- [63] B. Qi, S.Q. Zhang, S.Y. Wang, J. Meng, T. Koike, Phys. Rev. C 83 (2011) 034303.
- [64] B. Qi, H. Jia, N.B. Zhang, C. Liu, S.Y. Wang, Phys. Rev. C 88 (2013) 027302.
- [65] A. Bohr, B.R. Mottelson, Nuclear Structure, vol. II, Benjamin, New York, 1975.
- [66] F.Q. Chen, Q.B. Chen, Y.A. Luo, J. Meng, S.Q. Zhang, Phys. Rev. C 96 (2017) 051303.
- [67] E. Streck, Q.B. Chen, N. Kaiser, U.-G. Meißner, Phys. Rev. C 98 (2018) 044314.
- [68] P. Ring, P. Schuck, The Nuclear Many Body Problem, Springer Verlag, Berlin, 1980.
- [69] Q.B. Chen, S.Q. Zhang, P.W. Zhao, R.V. Jolos, J. Meng, Phys. Rev. C 87 (2013) 024314.
- [70] Q.B. Chen, S.Q. Zhang, P.W. Zhao, R.V. Jolos, J. Meng, Phys. Rev. C 94 (2016) 044301.